Available online at www.sciencedirect.com

SCIENCE DIRECT

Cement and Concrete Research 35 (2005) 1724 – 1733

Cement and Concrete Research

# Prediction of the hydraulic diffusivity from pore size distribution of concrete

Bulu Pradhan[a], M. Nagesh[b], B. Bhattacharjee[c,*]

[a]Department of Civil Engineering, Indian Institute of Technology, Delhi, Newdelhi-110 016, India
[b]School of Building Science and Technology, CEPT, K. L. Campus, Navarangpura, Ahmedabad-380 009, India
[c]Department of Civil Engineering, Indian Institute of Technology, Delhi, Hauz Kauz, New Delhi-110 016, India

Received 18 March 2003; accepted 20 October 2004

**Abstract**

A model is presented in this work through which variation of hydraulic diffusivity of concrete with relative water content can be obtained from pore size distribution as an input. The specific water capacity and hydraulic conductivity of concrete are expressed in terms of pore size characteristics, considering laminar flow due to capillary suction through tortuous elliptic tubes, oriented equally in three orthogonal directions. Hydraulic diffusivity being the ratio of hydraulic conductivity and specific water capacity is thus expressed in terms of pore size characteristics. The input pore size distributions have been determined experimentally for normal strength concrete mixes through mercury intrusion porosimetry. Using the model the variation of hydraulic diffusivity with relative water content is determined for three cases viz. 1) ideal continuous wetting, 2) ideal continuous drying and 3) random access of pores by water. These results are then compared with an experimentally obtained variation.


*Keywords:* Diffusivity; Pore size distribution; Porosity; Model; Hydraulic conductivity

## 1. Introduction

Deterioration of concrete is largely mitigated by ingress of water through it. Most of the reactions which result in deterioration of concrete take place in the presence of water. Thus the ingress of water is a necessary precondition for the deterioration and the degradation of concrete structures in service. This fact has been recognized for a long time and hence permeability and absorption tests are adopted for durability performance appraisal of concrete structures [1,2]. Essentially, these tests provide only qualitative information regarding durability performance. However, for service life prediction, often it is necessary to estimate the moisture content profile within the concrete structure at different ages during its service life. Moisture profile may include both vapor phase and liquid phase. In case of rain penetration and partially submerged structures, the ingress of water in liquid phase plays a dominant role [3]. The ingress of water into concrete is governed by the theory of unsaturated flow through porous media in general and the generalized Darcy's law for unsaturated flow in particular [4]. The material coefficient that is encountered in such modeling is the hydraulic diffusivity $D(\theta)$ and plays an important role in the context of water ingress in concrete. The ingress of water and the migration of fluid into concrete in general, take place through an interconnected pore system. Thus porosity and pore size distribution of concrete governs its permeation properties including hydraulic diffusivity [5].

In this work a model for hydraulic diffusivity is presented, in which the input data is the pore sizes and their corresponding cumulative pore volumes. The pore sizes and their corresponding cumulative pore volumes, which represent the pore size distribution, were experimentally determined through mercury intrusion porosimetry for

* Corresponding author. Tel.: +91 11 2659 1193; fax: +91 11 2658 1117.
*E-mail addresses:* bishwa@civil.iitd.ernet.in, bishwa_b@hotmail.com (B. Bhattacharjee).

0008-8846/$ - see front matter 
doi:10.1016/j.cemconres.2004.10.043

five concrete mixtures. In addition, hydraulic diffusivities of the same concrete mixes were also determined experimentally. Using the experimental pore size distribution data as input, hydraulic diffusivities at various relative water contents are obtained for two cases, namely; 1) when the pores are filled starting from largest sized pore first, followed by smaller size pores progressively with increase in water content, such that least water content corresponds to the largest pores; 2) when the saturated pores are emptied starting from the largest sized pores first followed by the emptying of smaller sized pores progressively as the water content decreases, such that least water content corresponds to the smallest size pores remaining filled. These two conditions correspond to the ideal continuous wetting and ideal continuous drying conditions respectively. However, in actuality, concrete pores are likely to be encountered by water in a random sequence. Hence a realistic simulation model for computation of hydraulic diffusivity is presented, whereby it is assumed that pores of various sizes are occupied by water in a random manner. The variation of hydraulic diffusivity with relative water content for 30 such random sequences of pore filling is thus obtained. The results obtained for three cases namely; 1) ideal continuous wetting 2) ideal continuous drying and 3) random access of pores by water are then compared with the experimentally determined variations of hydraulic diffusivity with relative water content.

## 2. Model development

### 2.1. Water ingress in unsaturated porous media and hydraulic diffusivity

Water ingress in unsaturated porous media is governed by unsaturated flow theory [4,6]. An extension of Darcy's law to unsaturated porous media results in the following equation. The vector flow velocity '$u$' is given by,

$$u = -k(\theta)\nabla \Phi \tag{1}$$

$\nabla \Phi$, is the hydraulic potential gradient and may include both capillary suction and gravitational components. $k(\theta)$ is a water content dependent hydraulic conductivity. $\theta$ is the water content. Hence by condition of continuity,

$$\frac{\partial \theta}{\partial t} = -\nabla \cdot u = \nabla[k(\theta)\nabla \Phi] \tag{2}$$

Where, $t$ is the time. In a horizontal one-dimensional flow-system, neglecting gravitational head, the hydraulic potential head $\Phi$ is the same as the capillary suction head $\psi$. Eq. (2) reduces to [4,6,7]:

$$\frac{\partial \theta}{\partial t} = \frac{\partial}{\partial x}\left[k(\theta)\frac{\partial \psi}{\partial x}\right] \tag{3}$$

where $x$ is space co-ordinate along horizontal direction, $(\partial\psi/\partial x)$ is the capillary suction head gradient and as suction depends upon water content, the same can be expanded by chain rule of differentiation as follows,

$$\frac{\partial \psi}{\partial x} = \frac{\partial \psi}{\partial \theta} \times \frac{\partial \theta}{\partial x}. \tag{4}$$

Variation of capillary suction with water content is not unique and differs depending on whether the material is being wetted from an initial dry state or is being dried from an initial saturated state, thus hysteresis is generally observed. However, considering continuous wetting or continuous drying situations, the relationship is generally unique. Thus in the above equation, $(\partial\theta/\partial x)$ is the wetness gradient and $(\partial\psi/\partial\theta)$ is the reciprocal of the specific water capacity $c(\theta)$ that is given by:

$$c(\theta) = \frac{d\theta}{d\psi} \tag{5}$$

Eq. (1) can be rewritten and analogous to Fick's law of diffusion, a term called hydraulic diffusivity $D(\theta)$ can be introduced as shown in Eqs. (6) and (7) respectively [6,8],

$$u = -k(\theta)\frac{\partial \psi}{\partial x} = -\frac{k(\theta)}{c(\theta)} \times \frac{\partial \theta}{\partial x} \tag{6}$$

$$D(\theta) = \frac{k(\theta)}{c(\theta)} = k(\theta)\frac{d\psi}{d\theta} \tag{7}$$

$D(\theta)$ is thus defined as the ratio of hydraulic conductivity to the specific water capacity and as both of these are functions of $\theta$, the hydraulic diffusivity must also be a function of $\theta$.

### 2.2. Porous material model for concrete

Concrete is a porous material consisting of gel pores and capillary pores. Gel pores are smaller in size with majority being smaller than $10^{-8}$ m. Capillary pores are larger in size and range from $10^{-8}$ to $10^{-5}$ m [9]. Only the capillary pores contribute towards the movement of water through concrete [10]. The capillary pores present in concrete are of irregular cross-sectional shapes and varies in size. Further, they are tortuous in nature, generally interconnected and randomly oriented. For the purpose of modeling the hydraulic diffusivity, the cross-section of these capillary pores can be assumed to be elliptical, i.e., varying from circular to slit with aspect ratio ranging from unity to a very large value. One third of the pores can be assumed to be oriented along each orthogonal direction. Water permeable porosity of such a system can be defined as:

$$p = \frac{N\pi l_c \alpha r_m^2}{V} = \frac{1}{V}\int_{r_{min}}^{r_{max}} \frac{dv}{dr}dr \tag{8}$$

where, $N$ is the number of pores in volume $V$, $l_c$ is the mean tortuous length of the capillary, $\alpha$ is the mean representative aspect ratio, $r$ is the pore size measured as half pore width (semi-minor axis of the elliptic pore), $r_m$ is the mean pore size, limits $r_{max}$, $r_{min}$ represent the maximum and minimum pore sizes respectively, $v$ is the cumulative pore volume and

$V$ is the total volume of the material. The differential pore size distribution ($\mathrm{d}v/\mathrm{d}r$) can be obtained when the cumulative pore volume versus pore size curve is available.

### 2.3. Water content and pore size distribution

The water content of a porous concrete can be related to the pore space it occupies and hence can be expressed in terms of differential pore size distribution ($\mathrm{d}v/\mathrm{d}r$) per unit dry mass of the concrete as [11,12],

$$\theta = -\rho \int_{r_1}^{r_2} \frac{\mathrm{d}v}{\mathrm{d}r}\mathrm{d}r. \tag{9}$$

The negative sign in Eq. (9) indicates a decrease in cumulative pore volume with increase in pore size. $r_1$ and $r_2$ in the above equation are the appropriate limits of integration within which all the pore sizes ranging from those greater than pore size $r_1$ to those smaller than pore size $r_2$ are filled with water. $\rho$ is the density of water. It is assumed that all the pores of sizes ranging from $r_1$ to $r_2$ are completely filled with water at the particular water content $\theta$. In case of horizontal flow in capillary porous media, the water flows under the action of capillary suction. The suction is created by surface tension force and flow takes place from a zone where capillary menisci are less curved to where they are more curved i.e. from a zone of lower suction to higher suction. In unsaturated concrete, assuming a continuous wetting situation, starting from a completely dry condition, the concrete would be partially saturated at a point away from the water source where waterfront is advancing in horizontal flow under capillary suction. The rate of entry of water into a capillary of radius $r_t$ at a distance $x$ from the source, according to Washburn's equation is given by [12,13]:

$$u_1 = \frac{\mathrm{d}x}{\mathrm{d}t} = \frac{r_t \sigma_w \cos\phi}{4x\mu} \tag{10}$$

where $u_1$ is the velocity, $\sigma_w$ is the surface tension of water, $\phi$ is the contact angle and $\mu$ is the viscosity of water. Converting the above differential equation to algebraic equation by variable separable method leads to the following expression:

$$r_t = \frac{2x^2\mu}{t\sigma_w \cos\phi} \tag{11}$$

where, $r_t$ is the radius of the continuous tube, in which water spreads at its length $x$ from the source, at time $t$. As in Eq. (11) $r_t$ is inversely proportional to $t$, at time $t$, at the point $x$ distance away from the source, water, having entered earlier in the larger pores, would occupy the pores having pore sizes ranging from $r_t$ to all pores having larger radii. At saturation the $r_t$ would correspond to the minimum pore size. Therefore for a continuous wetting process, the water content at a section is given as follows;

$$\theta(r) = -\rho \int_{r}^{r_{max}} \frac{\mathrm{d}v}{\mathrm{d}r}\mathrm{d}r \tag{12}$$

In case of continuous drying process from saturated condition, evaporation takes place from the surface at the wet bulb temperature. So long as the water content in the material at its surface is above the critical water content, during constant drying rate period the flow of water within the material takes place under capillary suction [14]. Consequently dehydration of water occurs in sequence of size from large capillary to smaller capillaries [6,14]. As the hydraulic diffusivity is the main consideration in this work, only liquid water transport process is considered. Therefore for continuous drying process the water content at a section can be expressed through Eq. (12) itself by changing the limits of integration to $r_{min}$ to $r$ instead of $r$ to $r_{max}$.

### 2.4. Capillary suction and pore size distribution

For a cylindrical tube of circular cross-section of radius $r'$ the capillary suction for horizontal flow of water can be written as [13,15];

$$P = \frac{2\sigma_w \cos\phi}{r'}. \tag{13}$$

However, for the assumed elliptic pore system, the modified equation for capillary suction can be obtained by equating the work done by suction pressure P with that done by the component of surface tension force along the direction of spread of water as follows;

$$P = \frac{\varepsilon\sigma_w \cos\phi}{\pi\alpha r^2} \tag{14}$$

The corresponding suction head is given in Eq. (15).

$$\psi = \frac{P}{\rho g} = \frac{\varepsilon\sigma_w \cos\phi}{\pi\rho g\alpha r^2} \tag{15}$$

where, $\varepsilon$ is the circumference of the elliptic pore, $g$ is the acceleration due to gravity and $r$ represents the pore size at which water spreads. Value of $\varepsilon$ can be computed by evaluating the appropriate elliptic integral when $\alpha$ and $r$ is known [16,17] and is given as $4\alpha rf$. $f$ depends on the aspect ratio $\alpha$ and is independent of $r$. When the pore system consists of continuous capillary pore sizes ranging from a smallest size to a maximum, as is the case under consideration, the rate of change of capillary suction with pore size can be obtained by differentiating the above equation with respect to '$r$'. It follows thus;

$$\frac{\mathrm{d}\psi}{\mathrm{d}r} = -\frac{4f\sigma_w \cos\phi}{\pi\rho g r^2} \tag{16}$$

Further by the chain rule of differentiation,

$$\frac{\mathrm{d}\psi}{\mathrm{d}\theta} = \frac{\mathrm{d}\psi}{\mathrm{d}r} \times \frac{\mathrm{d}r}{\mathrm{d}\theta} \tag{17}$$

Again by differentiating $\theta$ with respect to $r$ in Eq. (9) one can obtain;

$$\frac{\mathrm{d}\theta}{\mathrm{d}r} = -\rho\frac{\mathrm{d}v}{\mathrm{d}r} \tag{18}$$

Thus, as $(\mathrm{d}r/\mathrm{d}\theta)$ can be expressed in terms of pore size characteristics, then reciprocal of specific water capacity and, hence, specific water capacity itself, can also be expressed in terms of pore size distribution characteristics. Combining Eqs. (16) and (18), Eq. (17) can be rewritten as:

$$\frac{\mathrm{d}\psi}{\mathrm{d}\theta}=\frac{4f\sigma_{\mathrm{w}}\cos\phi}{\pi r^2\left(\frac{\mathrm{d}v}{\mathrm{d}r}\right)\rho^2 g}. \tag{19}$$

To express $D(\theta)$ completely in terms of pore size characteristics, it is necessary to express $k(\theta)$ also in terms of the same.

### 2.5. Hydraulic conductivity and pore size distribution

In unsaturated condition the water gets transported only through the water occupied pore spaces and the same pores contribute towards hydraulic conductivity. The expression for hydraulic conductivity can be obtained from the equation of stabilized laminar flow of an incompressible fluid through a cylindrical pipe of elliptic cross-section as given below for $j$th capillary [18].

$$u_j=\frac{\pi\alpha_j^3 r_j^4\Delta P}{4\mu l_{cj}\left(1+\alpha_j^2\right)}. \tag{20}$$

Since the flow takes place under capillary suction, $\Delta P$ can be replaced by $\rho g\Delta\Psi$. Here $\Delta\Psi$ is the small change in suction head. Further introducing space dimension d$x$, and the tortuosity $\tau_{\mathrm{j}}$, i.e. the ratio of tortuous length of capillary to the length of the material, Eq. (20) can be rewritten as;

$$u_j=\frac{\pi\alpha_j^3 r_j^4\rho g}{4\mu\tau_j\left(1+\alpha_j^2\right)}\times\frac{\Delta\psi}{\mathrm{d}x} \tag{21}$$

Considering the flow through unit cross-sectional area of the concrete, the number of pores per unit area of cross-section is equal to $N'$ and from Eq. (8), is given by:

$$N'=\frac{p\mathrm{d}x}{\pi\alpha_j r_j^2 l_{cj}} \tag{22}$$

Then the total flux per unit area is the sum of all the fluxes through all the tubes which are water filled. Summation of $u$ with varying $\tau$, $\alpha$ and $r$ is relatively complex, besides summation of $r$ with higher exponent (two or more) results in overestimation of contribution due to larger pores to hydraulic conductivity [10]. Therefore, assuming all water filled pores of uniform size, shape and tortuosity represented by their respective representative value, Eq. (21) can be multiplied by $N'$ to obtain the total flux per unit area. From the definition of hydraulic conductivity according to Darcy's law, using $N$' from Eq. (22) and taking the effect of orientation, results in the following expression for water content dependent hydraulic conductivity $k(\theta)$.

$$k(\theta)=\frac{pr_{\mathrm{m}}^2\rho g}{12\mu\tau^2(1+1/\alpha^2)} \tag{23}$$

$\tau$ is the mean tortuosity. Since the pore sizes vary logarithmically, hence instead of using simple mean the mean pore size $r_{\mathrm{m}}$ can be taken as mean distribution pore size as given in Eq. (24) [19,20].

$$\ln r_{\mathrm{m}}=\frac{\sum_{i=1}^{i=n}v_i\ln r_i}{\sum_{i=1}^{i=n}v_i}. \tag{24}$$

In the above equation $v_i$ is the incremental cumulative pore volume corresponding to $i$th pore size range, represented by geometric mean pore size $r_i$ of the size interval. Combining Eqs. (7),(19),(23) a relationship between hydraulic diffusivity and pore size distribution parameters can be obtained, as shown in Eq. (25).

$$D(\theta)=\frac{f\sigma_{\mathrm{w}}\cos\phi\times p_j r_{\mathrm{m}j}^2}{3\pi\rho\mu\tau^2 r_j^2\left(\frac{\mathrm{d}v}{\mathrm{d}r}\right)_j(1+1/\alpha^2)}. \tag{25}$$

The water content at a specific pore size $r_j$ can be obtained through Eq. (9) and the saturation water content can be obtained by changing the limits of integration in the same equation from $r_{\min}$ to $r_{\max}$. Then the relative water content can be determined as the ratio of the water content at a specific pore size to the saturation water content. The corresponding $D(\theta)$ can be obtained through Eq. (25). Hence the variation of $D(\theta)$ with relative water content can be obtained.

### 2.6. Model implementation

The main input to the model is the pore size distribution curve. Standard values are adopted for other inputs namely; surface tension of water: 0.0727 N/m at 20 °C; contact angle for water: 0°; dynamic viscosity of water: 0.001 N-s/m$^2$ at 20 °C and density of water: 1000 kg/m$^3$. The cumulative pore volume versus pore size curve can be obtained through mercury intrusion porosimetry (MIP), although there are other methods such as back-scattered electron (BSE) imaging technique is also available [21]. Intrusion of mercury in MIP and ingress of water in concrete are governed by the same equation, except that in MIP, mercury is forced into the pore under applied pressure, while in the case of water, developed suction pressure itself is responsible for the spread of water through the capillaries. Both intrusion of mercury in MIP and ingress of water under suction depend on accessibility and interconnectivity of pores. The correction for the assumed cross-section shapes of the pores can be taken in to account in MIP [22]. Ratio of circumference to the cross-section area for an elliptical pore of unit pore size $(4f/\pi)$ depends upon the aspect ratio and represents the influence of aspect ratio on suction. The same is also the multiplying correction factor for shape that can be applied to the pore radii obtained through MIP to convert the circular to elliptic shape of the cross-section of the pore. This factor varies from 2 for circular cross-section to 1 for slit. Assuming equal probabilities for all the possible shape a value of 1.5 can be adopted for the representative value of this factor. The value of 1.5 corresponds to an aspect ratio of nearly 2 and the same is assumed as the mean representative aspect ratio $\alpha$ for the model. Experimental and theoretical values of tortuosity have been reported in literature for particulate systems consisting of 2 mm spheres for different packing arrangements [11]. For random packing the value suggested is 2.1. For a uniformly random porous media a value $(\pi/2)^2 \approx 2.47$ has been proposed for tortuosity of cement based material by Maekawa et al. [8], and the same value is also adopted in this work as well. For an ideal pore system with pores of any given size isolated from other pores in such a way that there is no inter connection amongst pores of different sizes, in case of continuous wetting, the pores would fill sequentially from larger pore-sizes to smaller. This case is referred as ideal continuous wetting. The hydraulic diffusivity for such a situation is calculated using Eq. (25) from experimentally determined cumulative pore size curve through MIP and presented later. The experimentally obtained cumulative intrusion volume versus pore radius (circular cross-section) curve is taken as the input. The corrected pore size values for the assumed aspect ratio are taken and divided to a number of finite ranges starting from $r_1$, $r_2 \ldots r_n$ etc., such that $r_1$ and $r_n$ correspond to $r_{\min}$ and $r_{\max}$ respectively. The corresponding cumulative intrusion volumes are $v_1$, $v_2 \ldots v_n$. The $(dv/dr)$ value for each interval is thus calculated. For the ideal wetting situation starting from the interval $r_n - r_{n-1}$ when water enters the pore of size $r_{n-1}$, the suction is related to pore size $r_{n-1}$ and in calculation of $D(\theta)$ through Eq. (25), $(r_{n-1})^2$ appears in the denominator. $p_j$ in Eq. (25) is calculated as the sum of contribution of all pore sizes larger than $r_{n-1}$, i.e. using the limits of integration in Eq.(8) from $r_{n-1}$ to $r_n$. Correspondingly, $r_{mj}$ is also calculated through Eq. (24) in a similar manner for pore sizes larger than $r_{n-1}$. For any $j$th pore size thus the $D(\theta)$ is calculated using the same procedure till $r_1$. The water content $\theta$ corresponding to $j$th pore size is calculated using the lower and upper limits of integration in Eq. (9) as $r_j$ and $r_n$ respectively. The case of ideal drying is dealt with exactly in the same manner as those above except that the starting pore size interval here is $r_1$ to $r_2$, and $(r_2)^2$ appears in the denominator in Eq. (25). For drying at a higher water content through the interval $r_{j-1}$ to $r_j$, $r_j^2$ appears in the denominator and $p_j$ and $r_{mj}$ are calculated for all pores smaller than pore size $r_j$ using Eqs. (8) and (24) respectively. The water content is calculated using Eq. (9) with the lower and upper limits of integration as $r_1$ and $r_j$ respectively. In both of the above cases it is assumed that the pores of a given size is isolated from all other pore sizes, in real situation pores of all sizes are inter connected and size of a pore may also vary from a smaller to a larger value or vice-versa from point to point. Thus water may not be filled or withdrawn from pores in a sequential manner as assumed, rather water is likely to be filled or withdrawn in random sequence of pore sizes. The random sequence of pore size intervals is generated through a simulation procedure, by generating a set of uniform random number between 0 and 1. Multiplying the generated random number with the total number of intervals and rejecting the repetitions after rounding off to a whole number, a sequence of intervals is obtained. The water ingress in concrete can be assumed to follow the simulated sequence as obtained instead of in a sequence of continuously increasing or decreasing sizes. The intervals $(r_1 - r_2)$, $(r_2 - r_3) \ldots (r_{n-1} - r_n)$ is replaced accordingly with new sequences. The hydraulic diffusivity at a water content corresponding to the $j$th interval in the sequence is calculated through Eq. (25). $r_j$ in the equation corresponds to the upper limit of the pore size in the $j$th interval. $p_j$ is the porosity and is the ratio of $\Sigma dv$ to the total volume. Corresponding mean distribution pore size $r_{mj}$ is the geometric mean of the pore sizes for the intervals from 1 to $j$ in the random sequence. Similarly the corresponding water content is also obtained through the sum $\Sigma dv$ calculated as above and the hydraulic diffusivity over the complete range of relative water content is thus obtained. Incidentally the random sequence may correspond to both ingress as well as withdrawal of water. Thirty such sequences are generated to obtain the probable variation of hydraulic diffusivity with relative water content for experimentally determined pore size distribution of concrete and are presented later.

## 3. Experimental inputs and results

### 3.1. Mix proportions and specimen preparation

The mix proportions of five concrete mixes are given in Table 1. Ordinary Portland cement and reddish land quarried sand confirming to zone-II classification of British standard and potable laboratory tape water was used as fine aggregate and mixing water respectively. Graded coarse aggregates of 12 mm maximum size of quartzite origin were used with the ratio of fine aggregate to coarse aggregate as 1:2 by mass. Three specimens of sizes 50 mm × 50 mm × 300 mm, rectangular prism shape, were cast from different designed concrete mixes as replicates. The specimens were com-

Table 1
Mix parameters

| Mix | Cement content ($kg/m^3$) | Water–cement ratio | Aggregate–cement ratio |
|---|---|---|---|
| Mix 1 | 250 | 0.6 | 8.4 |
| Mix 2 | 350 | 0.4 | 5.7 |
| Mix 3 | 350 | 0.6 | 5.5 |
| Mix 4 | 350 | 0.8 | 5.3 |
| Mix 5 | 450 | 0.6 | 3.9 |

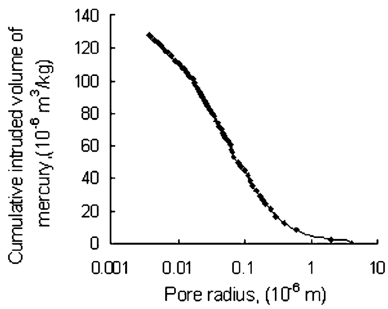


Fig. 1. Pore size distribution curve for 28 days cured specimens of mix 1.

pacted using a table vibrator. All the specimens were demouled after 24 h of casting and cured for 28 days in a curing tank at a temperature of 27±3 °C. After removing from the curing tank, the specimens were preconditioned by oven drying at 105–110 °C for 48 h and then cooled to room temperature (30±3 °C, with an average humidity of 50%) before testing.

### 3.2. Mercury intrusion porosimetry

Mercury intrusion porosimetry (MIP) was conducted on chunk concrete samples collected in a manner similar to that described in literature [23] from specimens cast with mixes shown in Table 1 ensuring the presence of at least one mortar aggregate interface in each. Three replicates were used in each mix. The samples were dried in an oven at a temperature of 105–110 °C for 48 h after 28 days of curing and stored in a desiccator over silica gel until tested. Correspondingly the surface tension of mercury and contact angle adopted are 0.484 N/m and 117° respectively. Testing was performed on Quantachrome Autoscan-33 porosimeter in the pressure range of sub-ambient pressure to 227 MPa (33,000 psi) covering a pore radius (circular cross-section) of $2\times10^{-9}$ m to 0.0002 m. [20,23,24]. The tests were performed at a constant moderate scanning rate and the cumulative intrusion versus the pore radius curve was obtained from the cumulative intrusion volume versus the pressure diagram obtained from the porosimeter using the Washburn equation given below. The averaging for three specimens was done by averaging the intruded volume at each radius for the three specimens to obtain the average intrusion volume versus pore radius curve.

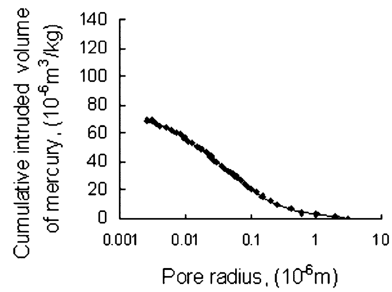


Fig. 3. Pore size distribution curve for 28 days cured specimens of mix 3.

$$r' = -\frac{2\sigma'\cos\phi'}{P'} \tag{26}$$

$r'$ is pore radius, $\sigma'$ is surface tension of mercury, $\phi'$ is the contact angle and $P'$ is the applied pressure. The cumulative volume versus pore size curves for the five concrete mixes thus obtained, are given in Figs. 1–5. The $r'$ values in these figures are multiplied with an appropriate correction factor for shape, to obtain pore size $r$ these are used in Eq. (25) for computation of $D(\theta)$.

### 3.3. Hydraulic diffusivity

When horizontal surface of a porous media is brought in contact with a water body such that there is negligibly small gravity head, for non-hygroscopic material the flow of water under capillary suction is governed by Eq. (3). The hygroscopic moisture content of concrete is very small compared to the total saturation moisture content and when in contact with water, flow under vapor pressure gradient can be neglected in comparison with the liquid water flow under suction. The water content at the solid–water interface would be saturation water content $\theta_s$. With interface as the origin, assuming the concrete specimen being a semi-infinite medium, the initial and boundary conditions are as follows. At, $t=0$, $\theta=\theta_i$, for all $x\geq0$. For $t>0$; at $x=0$, $\theta=\theta_s$, and $\theta=\theta_i$; at $x=\infty$. Applying Boltzmann's trans-

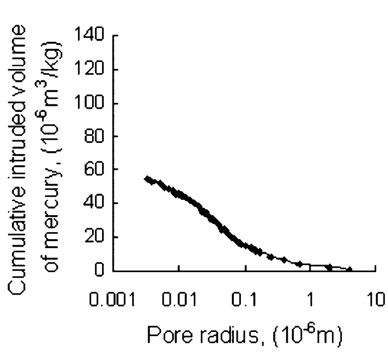


Fig. 2. Pore size distribution curve for 28 days cured specimens of mix 2.

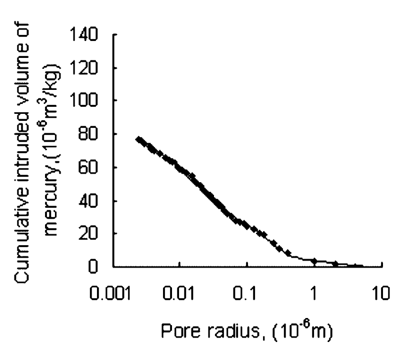


Fig. 4. Pore size distribution curve for 28 days cured specimens of mix 4.

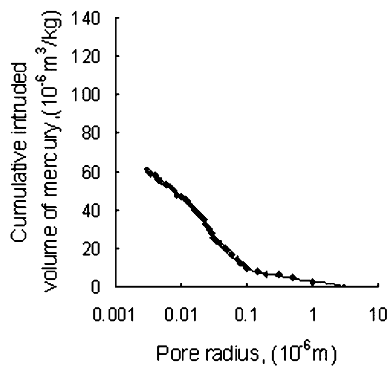


Fig. 5. Pore size distribution curve for 28 days cured specimens of mix 5.

formation, the partial differential Eq.(3) is reduced to an ordinary differential Eq. (27) given below [4,6,25–28]. Introducing the new variable $\eta = x.t^{-½}$ and transforming Eq.(3) in terms of $\eta$ results in

$$\frac{-\eta}{2} \cdot \frac{d\theta}{d\eta} = \frac{d}{d\eta}\left[D(\theta)\frac{d\theta}{d\eta}\right] \tag{27}$$

The above equation and the boundary conditions mentioned earlier provides for the method for determination of hydraulic diffusivity. The boundary conditions thus changes to: at $\eta=0$, $\theta=\theta_s$ and $\eta=\infty$, $\theta=\theta_i$; the last condition implies that at $\eta=\infty$, $d\theta/d\eta=0$. An approximate finite difference form of the Eq. (27) between $j$th and ($j$-1)th nodes on $\eta$ axis, can be written as follows [28];

$$-\frac{1}{\Delta\eta}\frac{1}{2}\eta_{(j-1/2)}\left[\theta_j - \theta_{(j-1)}\right] = \frac{1}{\Delta\eta}\left[\left\{D(\theta)\cdot\frac{d\theta}{d\eta}\right\}_j - \left\{D(\theta)\cdot\frac{d\theta}{d\eta}\right\}_{(j-1)}\right] \tag{28}$$

and a rearrangement of the same results in the following expression;

$$D(\theta)_j = \frac{\left[\left\{D(\theta)\cdot\frac{d\theta}{d\eta}\right\}_{(j-1)} - \frac{1}{2}\cdot\eta_{(j-1/2)}\left(\theta_j - \theta_{(j-1)}\right)\right]}{\left\{\frac{d\theta}{d\eta}\right\}_j}. \tag{29}$$

Thus from a plot of $\theta$ versus $\eta$ curve, $D(\theta)_j$ at the $j$th node can be obtained when $D(\theta)$ at the ($j-1$)th node and $d\theta/d\eta$ at $j$th and ($j-1$)th node are known. Considering the boundary condition at $\eta=\infty$, $\theta=\theta_i=\theta_1$ (initial water content) and $d\theta_1/d\eta=0$ (i.e. $t=0$ or $x=\infty$), $D(\theta)_2$ at a water content $\theta_2$ can be estimated as given below;

$$D(\theta)_2 = -\frac{\left[\frac{\eta_{1\frac{1}{2}}}{2}\cdot(\theta_2 - \theta_1)\right]}{\left\{\frac{d\theta}{d\eta}\right\}_2} \tag{30}$$

where node 1 represents the boundary $\eta=\infty$. $D(\theta)$ values at subsequent nodes i.e. at other higher water contents can now be estimated easily by a step by step procedure using Eq.

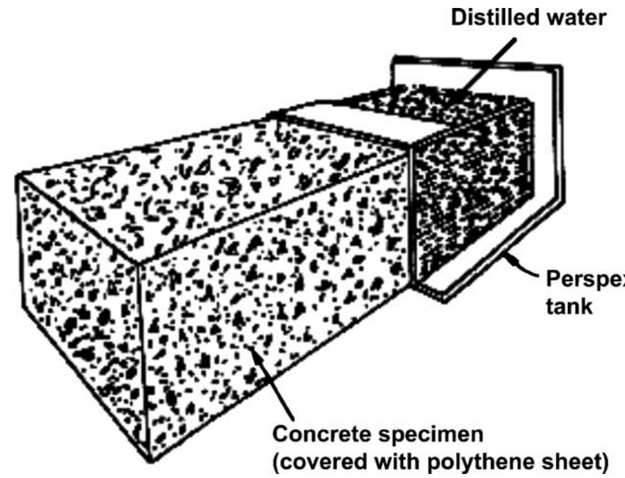


Fig. 6. Experimental arrangement for hydraulic diffusivity.

(29). The experimental arrangement is schematically shown in Fig. 6. The specimen is preconditioned by oven drying at 105–110 °C for 48 h and then cooled to room temperature as explained earlier. One end of the preconditioned specimen is exposed to distilled water kept in a plastic reservoir with its edges properly sealed. Further the specimen is wrapped with a polythene sheet to avoid evaporation of moisture from its surface. The specimen is then exposed to distilled water as shown in Fig. 6, for different pre-decided durations of exposure. The water content profile at various times and at different points along the length of the specimen due to the horizontal ingress of water was determined using a pre-calibrated in-situ moisture meter ($H_2O$ meter, James Non-Destructive Testing systems USA, model M-49). The instrument used in this experiment operates by measuring the dielectric constant i.e., permittivity of the material within the electromagnetic field produced by the instrument. The measured permittivity of the specimen is correlated to the water content of the material for its estimation. The calibration curve was obtained using a number of observations and attaining the moisture content both from dry state to saturation and from saturated state to air dried state. A calibration curve between measured meter readings and the actual water content, obtained through an oven drying procedure for concrete designated as mix 3 in Table 1 is shown in Fig. 7. Calibration curves had been obtained for all concrete mixtures and were used to determine the water content

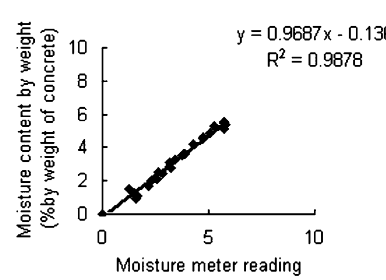


Fig. 7. Calibration curve between measured meter readings and the actual water content for mix 3.

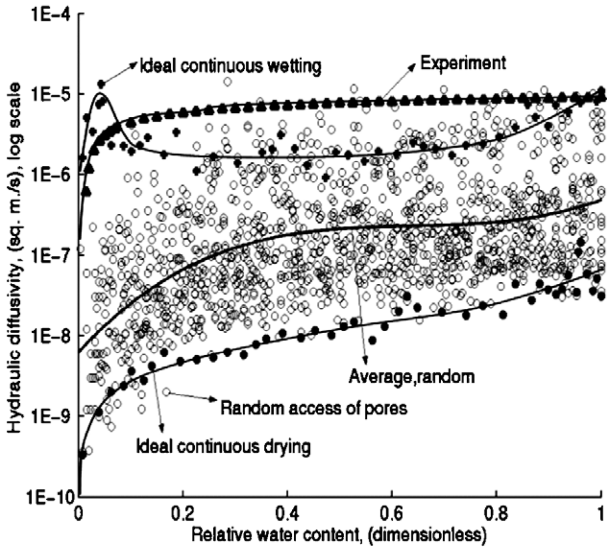


Fig. 8. Variation of hydraulic diffusivity with relative water content for mix 1.

profile in the specimen along the direction of water movement at various times. These calibration curves are linear as shown in Fig. 7 or are of exponential form as $Y = \mathrm{k1} \times \mathrm{e}^{\mathrm{k2} \times (X)} - 1$, where, $Y$ stands for percentage water content by mass of concrete and $X$ stands for natural logarithm of meter reading plus unity (as natural logarithm of zero is minus infinity). The square of the correlation coefficient i.e. $R^2$ varies for the calibration curves from 0.80 to 0.99. Using these calibration curves, plots of $\theta$ against $x$ at various time $t$ could be obtained and had been combined for the three replicates to obtain plots of $\theta$ versus $\eta$. Using these curves variation of hydraulic diffusivity with relative water content was then obtained by dividing the curves into finite intervals as explained earlier [26,28]. These results are presented in the following section together with the results obtained through the proposed model.

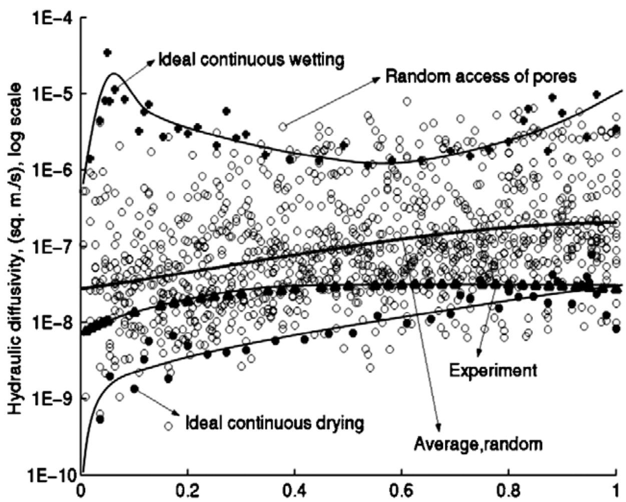


Fig. 9. Variation of hydraulic diffusivity with relative water content for mix 2.

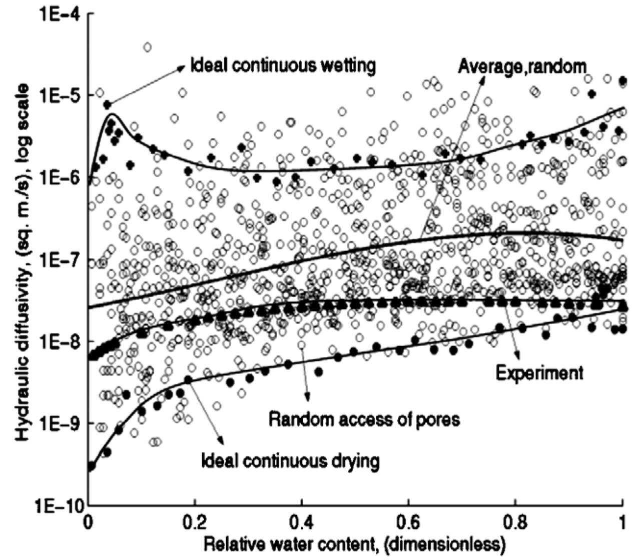


Fig. 10. Variation of hydraulic diffusivity with relative water content for mix 3.

### 3.4. Results

Using the pore size distribution curves presented in Figs. 1–5, the curves showing variation of hydraulic diffusivity with relative water content for the two cases namely, ideal continuous wetting and ideal continuous drying are obtained as described earlier and are presented in Figs. 8–12 respectively for mix 1 to mix 5. In addition the scatter of points representing the variation of hydraulic diffusivity with relative water content for random access of pores by water for 30 random sequences of pore sizes obtained through simulation procedure stated earlier are also shown in the same figures. A minimum numbers of 30 random sequences are required in order to avoid the statistical error due to small sample size. It has been observed that for a single random sequence of pore sizes this variation exhibits

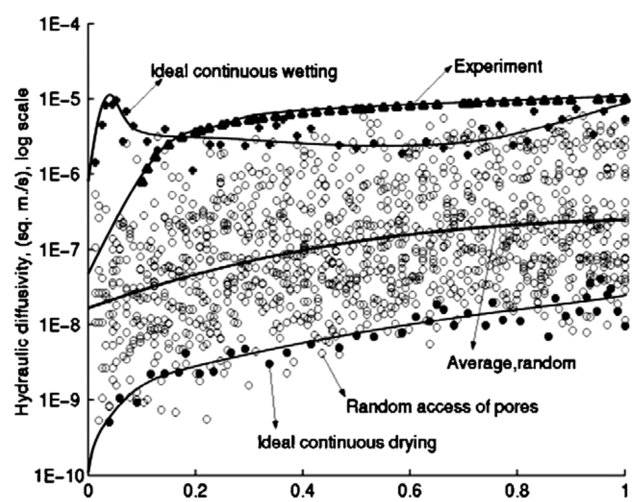


Fig. 11. Variation of hydraulic diffusivity with relative water content for mix 4.

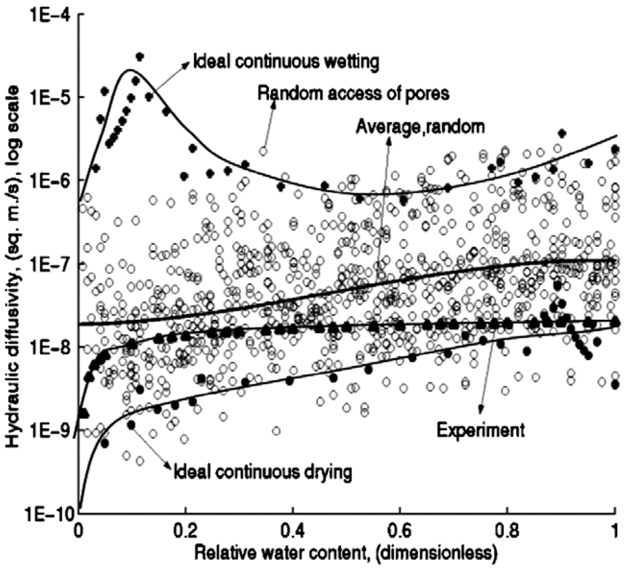


Fig. 12. Variation of hydraulic diffusivity with relative water content for mix 5.

large scatter. Average curve representing this variation for all 30 random sequences is also plotted along with ideal continuous drying and wetting curves. For the purpose of comparison, the experimentally obtained variations of hydraulic diffusivity with relative water content are further superimposed over theoretically obtained results in the same figures. For all the five mixtures, the wetting and drying curves do not follow the same path and the ideal continuous wetting curve lies above the drying one. Majority of the scattered points obtained for 30 random sequences of pore access lie within the bounds of ideal continuous wetting and drying curves and the average curve of these points lie approximately at the middle of these bounds. The experimental variation of hydraulic diffusivity with relative water content, lie mostly within the bounds of wetting and drying curves. However, these curves lie completely within the bounds of the scatter of points. Thus ideal continuous wetting and drying curves represent the practical upper and lower bounds respectively of hydraulic diffusivity. From Eq. (25), it is evident that at any water content, hydraulic diffusivity is directly proportional to porosity $p_j$ and square of mean pore size of water filled pores $r_{mj}$; and is inversely proportional to square of pore size $r_j$ at which water is either entering or receding and, the $(dv/dr)_j$ at the same $r_j$. $p_j$ increases with water content both in case of wetting as well as drying situations. Ratio of square of $r_{mj}$ to that of $r_j$ would increase with water content in case of wetting while $dv/dr$ is least in the beginning and increases slowly till a point where there is a sudden increase in its value at certain pore size ($r_j$), as evident from Figs. 1–5. This results in a sudden decrease of $D(\theta)$ from a peak after an initial increase in the case of wetting situation, thereafter followed by a gradual increase as $dv/dr$ tends to reduce slightly. In the case of drying situation, ratio of square of $r_{mj}$ to that of $r_j$ would decrease with water content and $(dv/dr)_j$ increases with water content, but the resultant decrease in $D(\theta)$ is counteracted by an increase in $p_j$. Thus $D(\theta)$ increases initially at a rapid rate but as $(dv/dr)_j$ increases to a maximum value, the rate of increase of $D(\theta)$ decreases. The trends of hydraulic diffusivity versus relative water content presented by various authors in the past for unsaturated soil, cement paste and similar other materials do not match with each other, i.e. there is not a single specific trend of hydraulic diffusivity versus relative water content [6,26,27,29,30]. Bruce and Klute [26] reported an increasing trend of natural logarithm of hydraulic diffusivity up to a certain water content for unsaturated soil followed by a decrease after an initial peak. Hillel [6] reported a similar trend for unsaturated soil except that the peak is followed by a decrease and a further steep increase. Hall [4] reported a linearly increasing relationship between natural logarithm of hydraulic diffusivity and relative water content. Gummerson et al. [29] reported a trend between logarithm of hydraulic diffusivity and relative water content for cement–lime–sand mortar through a nonlinear curve with high initial rate of increase of hydraulic diffusivity with relative water content followed by a low rate of increase. Fairhurst and Platten [30] also reported a similar trend for cement pastes. The differences in the reported trends for porous materials may be due to the variability introduced by the random access of the pores by water.

The water content profile in the concrete governs the progress of the degradation fronts. Therefore the same is required to be estimated and the values of hydraulic diffusivity obtained through the developed model can be useful in this regard. The degradation fronts in concrete progress in both wetting and drying cycles. During wetting higher values of hydraulic diffusivity would result in quicker wetting of the structures. Similarly, while drying smaller values of hydraulic diffusivity would result in longer duration of drying of the structures. In such a situation, adopting maximum value of hydraulic diffusivity for wetting situation and minimum value of hydraulic diffusivity for drying situation would lead to a longer cycle time of deterioration. This can therefore be referred to as a conservative approach with regards to wetting and drying in concrete structures in the context of service life prediction and can therefore be adopted for design purpose. Thus the hydraulic diffusivity values which are calculated for ideal continuous wetting and the ideal continuous drying situations, which also represent the upper and lower bounds, can be adopted in practice for wetting and drying conditions respectively.

## 4. Conclusions

1. In this work a model for prediction of hydraulic diffusivity of concrete with pore size distribution as input is presented and validated against experimental results.

2. Through this study, it has been found that the value of hydraulic diffusivity is more during wetting as compared to that during drying. The profile of hydraulic diffusivity with relative water content during wetting and drying represent the upper and lower bounds of hydraulic diffusivity. All the practical values of hydraulic diffusivity are likely to lie within these bounds including the experimentally obtained variation of hydraulic diffusivity with relative water content.
3. The upper and lower bounds proposed can be adopted in practice for predicting the water content profile in concrete during wetting and drying conditions respectively, in the context of service life prediction of concrete structures.

## References

[1] P.A.M. Basheer, A brief view of methods for measuring the permeation properties of concrete in-situ, Proceedings of the Institution of Civil Engineers: structures and buildings 99 (1) (1993) 74–83.
[2] J.H. Bungey, S.G. Millard, Testing of Concrete in Structures, Third ed., Chapman and Hall, 1996.
[3] C. Hall, A.N. Kalimeris, Water movement in porous building materials—V. Absorption and shedding of rain by building surfaces, Building and Environment 17 (4) (1982) 257–262.
[4] C. Hall, Water movement in porous building materials—I. Unsaturated flow theory and its applications, Building and Environment 12 (2) (1977) 117–125.
[5] R. Kumar, Strength and Permeation Quality of Concrete Through Mercury Intrusion Porosimetry, PhD thesis, Indian Institute of Technology Delhi, India, 1997.
[6] D. Hillel, Soil and Water, Physical Principles and Processes, Academic Press, New York and London, 1971.
[7] T.A. Carpenter, E.S. Davies, C. Hall, L.D. Hall, W.D. Hoff, M.A. Wilson, Capillary water migration in rock: process and material properties examined by NMR imaging, Materials and Structures 26 (1993) 286–292.
[8] K. Maekawa, R. Chaube, T. Kishi, Modelling of Concrete Performance, Routledge, London and New York, 1999.
[9] A.M. Brandt, Cement Based Composites: Materials, Mechanical Properties and Performance, E&FN Spon, UK, 1995.
[10] H.W. Reinhardt, K. Gaber, From pore size distribution to an equivalent pore size of cement mortar, Materials and Structure 23 (1990) 3–15.
[11] A.V. Luikov, Heat and Mass Transfer, Mir Publishers, Moscow, 1980.
[12] V.G. Gagarin, V.A. Mogutov, Unsteady movement of fluid in building materials, in: J.B. Chaddock, B. Todorovic (Eds.), Heat and Mass Transfer in Building Materials and Structures, Hemisphere Publishing Corporation, New York, 1991, pp. 43–62.
[13] A.W. Adamson, Physical Chemistry of Surfaces, Interscience Publishers, Inc., New York and London, 1960.
[14] R. Toei, Theoretical fundamentals of drying operation, Drying Technology 14 (1) (1996) 1–194.
[15] A. Volkwein, The capillary suction of water into concrete and the abnormal viscosity of the pore water, Cement and Concrete Research 23 (4) (1993) 843–852.
[16] M.L. Boas, Mathematical Methods in the Physical Sciences, John Wiley Sons, New York, 1983.
[17] M. Abramowitz, I.A. Stegun, Handbook of mathematical functions, Dover Publications Inc., New York, 1970.
[18] B. Yavorsky, A. Detlaf, Handbook of Physics, Mir Publishers, Moscow, 1977.
[19] C. Atzeni, U. Massidda, U. Sanna, Effect of pore size distribution on strength of hardened cement pastes, Proceedings of the First International RILEM Congress on Pore Structure And Material Properties, Paris, 1987, pp. 195–202.
[20] R. Kumar, B. Bhattacharjee, Porosity, pore size distribution and in situ strength of concrete, Cement and Concrete Research 33 (1) (2003) 155–164.
[21] S. Diamond, Mercury porosimetry—an inappropriate method for the measurement of pore size distributions in cement-based materials (a review), Cement and Concrete Research 30 (10) (2000) 1517–1525.
[22] R.A. Cook, K.C. Hover, Mercury porosimetry of cement-based materials and associated correction factors, ACI Materials Journal 90 (2) (1993) 152–161.
[23] M.A.I. Laskar, R. Kumar, B. Bhattacharjee, Some aspects of evaluation of concrete through mercury intrusion porosimetry, Cement and Concrete Research 27 (1) (1997) 93–105.
[24] R. Kumar, B. Bhattacharjee, Study on some factors affecting the results in the use of MIP method in concrete research, Cement and Concrete Research 33 (3) (2003) 417–424.
[25] J. Crank, The Mathematics of Diffusion, Clarendon Press, Oxford, 1956.
[26] R.R. Bruce, A. Klute, The measurement of soil moisture diffusivity, Soil Science Society of America Proceedings 20 (1956) 458–462.
[27] C. Hall, Water sorptivity of mortars and concrete: a review, Magazine of Concrete Research 41 (147) (1989) 51–61.
[28] M. Nagesh, B. Bhattacharjee, Modeling of chloride diffusion in concrete and determination of diffusion coefficients, ACI Materials Journal 95 (2) (1998) 113–120.
[29] R.J. Gummerson, C. Hall, W.D. Hoff, R. Hawkes, G.N. Holland, W.S. Moore, Unsaturated water flow within porous materials observed by NMR imaging, Nature 281 (1979 (Sept)) 56–57.
[30] D. Fairhurst, A.K. Platten, Moisture distributions and the hydraulic diffusivity of hardened cement pastes modified by partial replacement with condensed silica-fume, Proceedings of the International Conference on Maintenance and Durability of Concrete Structures (1997 (Mar 4–6)) 17–20.